Electrophoretic Sol-Gel Deposition

19

Atsunori Matsuda and Masahiro Tatsumisago

Contents

Abstract

The sol-gel method for particle preparation and electrophoretic deposition of the particles has been used to prepare thick films. This series of techniques, so-called electrophoretic sol-gel deposition, is reviewed. After brief description of principles of electrophoretic deposition, several examples of practical applications of electrophoretic sol-gel deposition are introduced, with silica thick films, for crack-free inorganic–organic composites, photonic crystals, and self-humidifying films; titania

A. Matsuda (✉)
Department of Electrical and Electronic Information Engineering, Toyohashi University of Technology, Toyohashi, Aichi, Japan
e-mail: matsuda@ee.tut.ac.jp

M. Tatsumisago
Department of Applied Chemistry, Osaka Prefecture University, Sakai, Osaka, Japan
e-mail: tatsu@chem.osakafu-u.ac.jp

L. Klein et al. (eds.), *Handbook of Sol-Gel Science and Technology*,
https://doi.org/10.1007/978-3-319-32101-1_14

thick films, for photocatalysts, and bio-related films; polysilsesquioxane thick films, for optical devices with high transmittance and micropatterns; and template-based oxide nanorods, for advanced and future applications.

Introduction

Electrophoretic deposition is a versatile process for formation of thin and thick films on substrates whereby electrically charged particles are deposited onto the substrates as an electrode from a stabilized suspension under a DC electric field (Sarker and Nicholson 1996). This process has widely been applied to various fields such as preparation of phosphors for displays, solid electrolytes for electrochromic displays, cathodes for lithium secondary batteries, superconductors, ferroelectric materials, and biomaterials (Mizuguchi et al. 1983; Kuwabara et al. 1991; Nojima et al. 1991; Nagai et al. 1993; Koura et al. 1995; Yamashita et al. 1998). The main advantage of the electrophoretic deposition is the fact that thick films can be prepared on various substrates with a complicated shape in much shorter time compared with the other coating techniques. The film thickness can be controlled by varying the preparation conditions such as applied voltage, deposition time, and concentration of the suspensions. In practice, however, the preparation of stable suspensions with fine and uniform particles, which is essential to obtain excellent thick films, is not so easy. For example, when raw materials are ground using a conventional ball mill, the shape of the particles is not uniform and the size distribution is broad. The sol-gel method permits the preparation of uniform, spherical, and fine particles. So-called electrophoretic sol-gel deposition, which is combined sol-gel method for particle preparation and electrophoretic deposition of the sol-gel derived particles, has been proposed as a promising procedure to prepare thick films (Kishida et al. 1994). In this chapter, the principle of the electrophoretic sol-gel deposition technique is described and the progress in research and technique is reviewed.

Preparation Processes

The electrophoretic sol-gel deposition technique is based on the preparation of particles from metal alkoxides by sol-gel method and the deposition of the sol-gel derived particles by electrophoresis.

Preparation of Particles by Sol-Gel Method

The formation of solid particles from solutions proceeds through nucleation and growth of hydrolyzed and condensed metal alkoxides. Various kinds of particles such as SiO_2, TiO_2, ZrO_2, Al_2O_3 can be prepared from corresponding metal alkoxides (Pierre 1998). Among these metal oxides, monodispersed SiO_2 particles are

well known to be obtained by Stöber process based on the growth of the primary particles by Ostwald ripening due to their large solubility of and great size-dependent solubility under basic conditions (Stöber et al. 1968; Iler 1979). Organosilsesquioxane ($RSiO_{3/2}$) microparticles, which are a kind of inorganic–organic hybrid with a Si–C covalent bond, have been also prepared from organotrialkoxysilanes (Katagiri et al. 1998). The particles formed in the solution are directly used for electophoretic deposition. However, centrifugation of the particles followed by redispersion in adequate solvents is preferred to obtain electophoretically deposited films depending on circumstances.

Deposition of Particles by Electrophoresis

Electrophoretic deposition process basically consists of three steps: (i) electrical charging of particles in a suspension (electrification), (ii) moving of the charged particles toward the oppositely charged electrode under a DC electric field (electrophoresis), and (iii) coagulation of the particles on the electrode to form a film (deposition). The surface charge on the particles in the suspension is characterized by the charge density and surface potential. The mechanism bf charging is explained either by the dissociation and ionization of the surface functional groups on the particles or by the adsorption of potential-determining ions on the particles. The charged particles attract oppositely charged ions to determine the zeta potential (Stern 1924).

Schematic drawing of the electrophoretic sol-gel deposition cell is shown in Fig. 1. When an external electric field is applied to the charged particles, the particles move in the suspension at an electrophoretic velocity determined by the balance between the electric field and the viscous forces which act on the particles (O'Brien and White 1978). With respect to the deposition process, several theoretical approaches have been done so far. Hamaker and Verwey (1940) proposed that deposition occurs via accumulation of particles at the electrode. They suggested that the phenomenon of electrophoretic deposition is identically the same as that of sedimentation. The accumulated particles close to the electrode are to be deposited because of the pressure that overcomes the interparticle potential barrier.

Constant-Voltage and Constant-Current Deposition. Constant-voltage (potentiostatic) and constant-current (galvanostatic) electrophoretic deposition techniques have been employed so far (Zhang et al. 1992).

In the constant-voltage electrophoretic deposition, the potential between the electrodes is maintained constant. The deposition of the accumulated particles requires a steeper potential than that the electrophoresis of the dispersed particles needs. Therefore, electrical resistance largely increases during the deposition. The current resulting from constant-voltage electrophoresis decreases as a function of the deposition time. The current decreases because the growing film continually increases the total cell resistance. The voltage drop in the film is equal to the product of the current and the film resistance. Therefore, the current reflects the changes in resistance due to physical and chemical properties of the films. The film will cease to

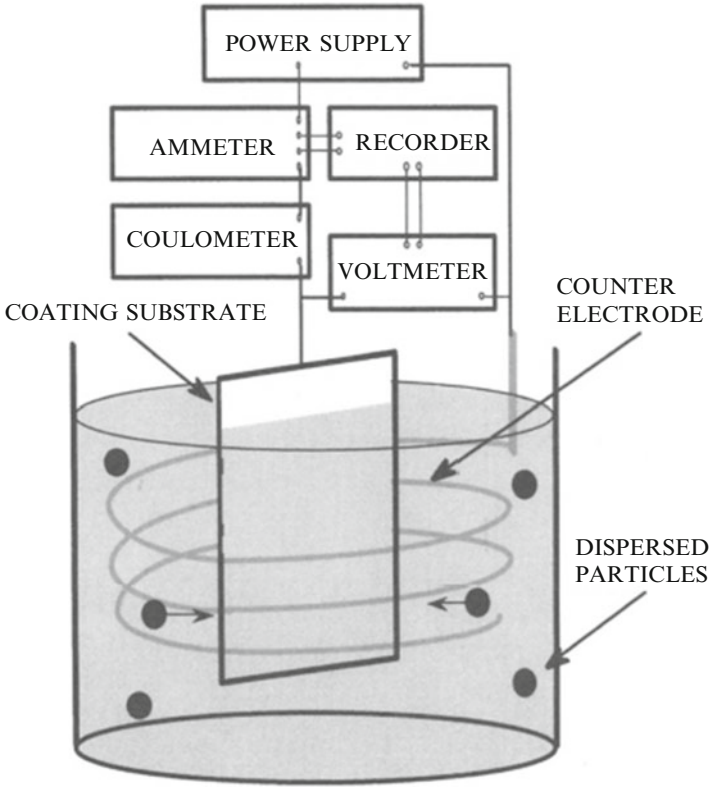

Fig. 1 Schematic drawing of the electrophoretic sol-gel deposition cell which illustrates the process

grow when the voltage drop of the film becomes equal to the constant applied voltage.

Under constant current electrophoretic deposition, the potential inducing electrophoresis is maintained constant by increasing the total potential drop between the electrodes. As a result, inhomogeneity in density, microstructure and morphology can be avoided. Constant current electrophoretic deposition provides a high deposition rate. Therefore, constant current electrophoretic deposition can avoid the limited deposition and deposition-rate problems in the constant-voltage process (Sarker and Nicholson 1996).

Solvent and Electrification. Aqueous and nonaqueous solvents have been used for the suspensions for the electrophoretic deposition. Although aqueous suspensions are harmless and cost effective, the formation of hydrogen gas at the cathode and oxygen gas at the anode through electrolysis of water results in the degradation of the resultant films (Ryan and Massoud 1979). In general, nonaqueous suspensions are preferential for the deposition of metal oxide films. Several kinds of organic solvents such as alcohol, acetone, acethylacetone, cyclohexanone have been

reported to be used for the preparation of thick films so far (Koura et al. 1995; Ishihara et al. 1996; Yamashita et al. 1997). The addition of small amounts of I_2 and water to ketone generates H^+ ions by a keto–enol tautomerism. The adsorption of H^+ ions to the metal oxide particles determines their zeta-potential and permits the electrophoretic deposition of the particles at the cathode.

Practical Applications

Silica Thick Films

Silica thick films have been prepared on a stainless steel sheet by the electrophoretic sol-gel deposition in the presence of sodium dodecyl sulfate (SDS) as dispersant in a sol containing silica particles (Nishimori et al. 1995, 1997). Silica particles were prepared by hydrolysis of tetraethoxysilane (TEOS) under basic conditions. SDS was dissolved in 0.5 mol dm^{-3} NH_3 aqueous solution, and TEOS was diluted separately with the same amount of ethanol (EtOH). These two solutions were mixed and stirred at 25 °C. The molar ratio of TEOS/H_2O/EtOH was fixed to be 0.2/10/10. The content of SDS was changed from 0 to 0.3 mass% against the total weight of the sols.

The size of silica particles and the geometrical standard deviation, σ_g, as a function of the content of SDS is shown in Fig. 2. The growth of the particles is completed in 12 h of the reaction time. Monodispersed silica particles with small σ_g (<1.1) are obtained when the content of SDS is up to 0.25 mass%. The value of σ_g is decreased with an increase of SDS. The particle diameter is increased from *ca*. 0.09 to *ca.* 1.2 μm with an increase of SDS (0–0.25 mass%). When the content of SDS is

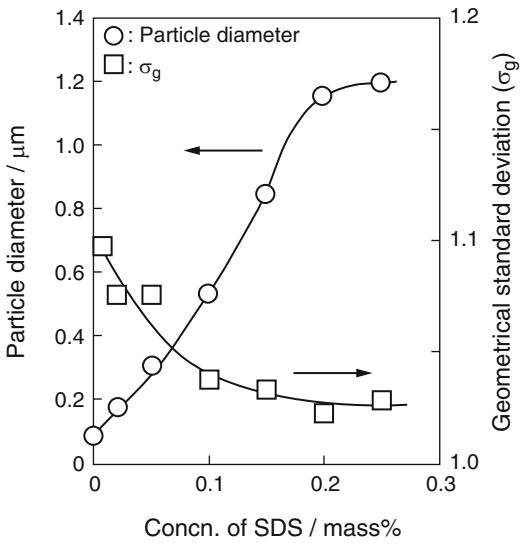

Fig. 2 Size of silica particles and the geometrical standard deviation, σ_g, as a function of the content of SDS (Nishimori et al. 1997)

larger than 0.3 mass%, the particles aggregate and monodispersed particles are not obtained. In this way, monodispersed silica particles with various particle sizes up to 1.2 μm in diameter are easily prepared by changing the amount of SDS.

SEM photographs of the particles extracted with different reaction periods are shown in Fig. 3. The content of SDS was 0.2 mass%. Double spherical particles by coalescence with an order of submicrometer in particle size are observed when reaction time is 30 min (Fig. 3a). The coalescence is not observed and spherical larger particles are finally obtained by stirring for 12 h (Fig. 3b). This indicates that the coalescence of the particles occurs in earlier reaction period and larger spherical particles are finally obtained.

The weight of silica films prepared by the electrophoretic sol-gel deposition using SDS-containing silica sol is shown in Fig. 4 as a function of applied voltage. The contents of SDS added were changed from 0 to 0.2 mass%. In the absence of SDS, the deposited films collapse in 10 min after withdrawing. On the other hand, the sols containing SDS yield thick films on the stainless steel sheets by the electrophoretic

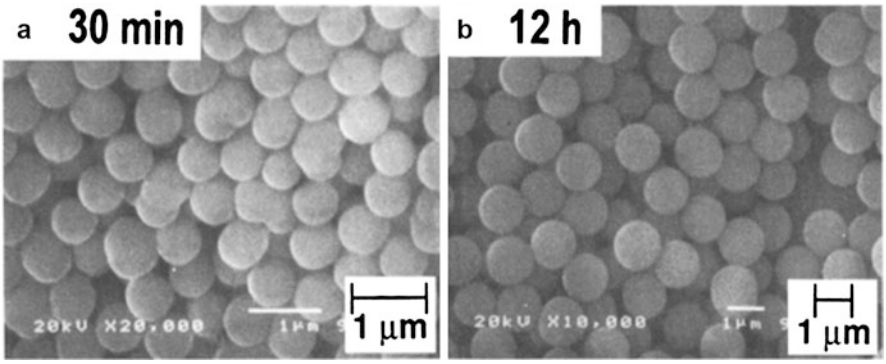

Fig. 3 SEM photographs of the silica particles extracted with different reaction periods: (**a**) for the particles with reaction time for 30 min and (**b**) for 12 h (Nishimori et al. 1997)

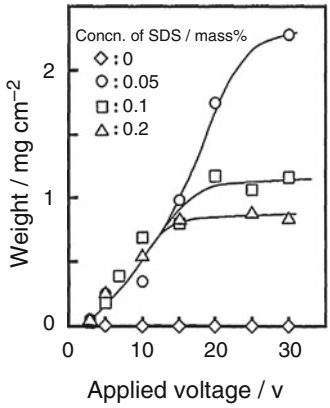

Fig. 4 Weight of silica films prepared by the electrophoretic sol-gel deposition using SDS-containing silica sol as a function of applied voltage. The contents of SDS added were changed from 0 to 0.2 mass% (Nishimori et al. 1995)

deposition. SDS depresses the film delamination during drying to permit the maximum thickness of 20 μm. This may be caused by the fact that SDS prevents the particles from aggregating excessively on the sheet in the electrophoresis because SDS is a typical dispersant. SDS also reduces the surface tension of the sols and prevents the film from cracking caused by the capillary force in the drying process. When SDS concentration is 0.05 mass%, the weight is increased with increasing voltage up to 30 V. If SDS concentrations are 0.1 and 0.2 mass%, the weight of the deposited films is gradually increased with increasing applied voltage in the same way under the applied voltage smaller than 15 V. However, the weight is saturated when the voltage is lager than 15 V. In these voltages, sedimentation of the particles is observed near the cathode during the electrophoresis of the sols. The addition of larger amount of SDS probably makes the sols unstable.

For preventing the microcracks, it is important to improve the adhesion of the particles as a constituent of the thick films. The addition of organic polymers in sols is expected to improve the adhesion of the particles and prevent the microcracks of the deposited films. Polycarboxylic acids are known to act as a useful binder in the preparation of green sheets from metal oxide particles. Polycarboxylic acids are also expected to be useful to prepare co-deposited films of the acid with particles by electrophoresis because they have a negative charge due to $–COO^-$ groups in basic conditions. Poly(acrylic acid) (PAA) is an effective binder since PAA contains a large number of carboxyl groups (Nishimori 1996a).

Using silica sols with the addition of PAA, films of *ca.* 25 μm in thickness are prepared on a stainless steel sheet with no cracks. SEM photographs of the surface of the silica thick films prepared without and with addition of 0.11 mass% PPA are shown in Fig. 5. Both films are prepared under an applied voltage of 10 V for 10 min.

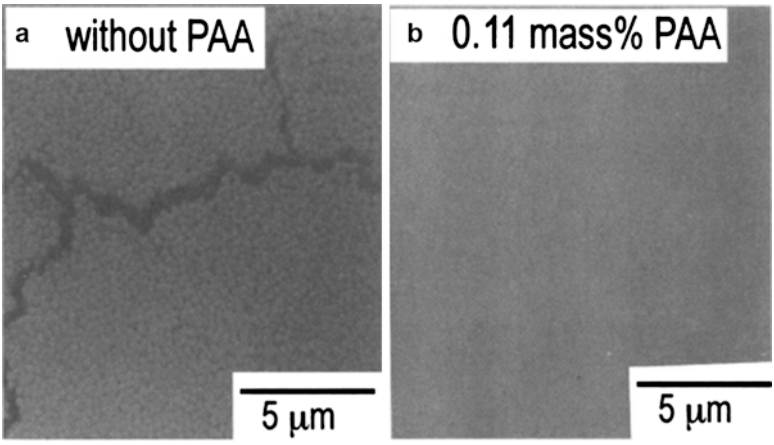

Fig. 5 SEM photographs of the surface of the silica thick films prepared without and with addition of 0.11 mass% PAA. Both films were prepared under an applied voltage of 10 V for 10 min (Nishimori 1996a)

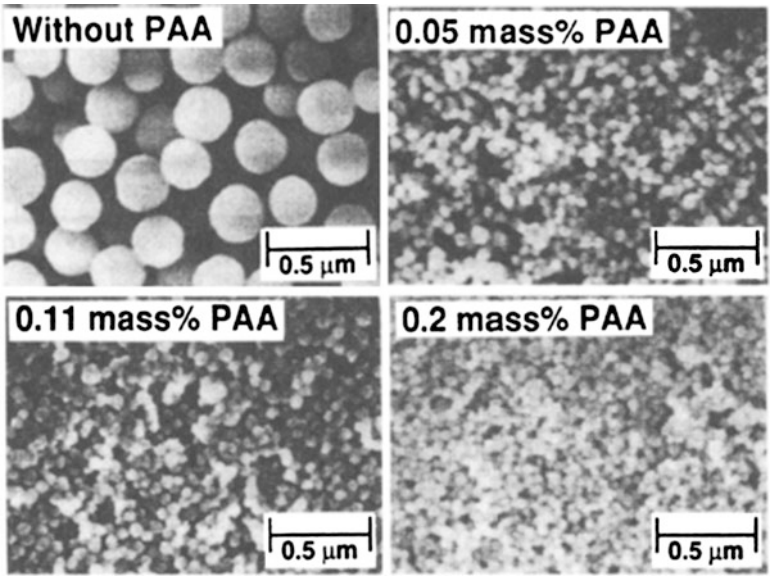

Fig. 6 SEM photographs of silica particles prepared with different amounts of PAA added (Nishimori 1996a)

Microcracks are observed in the films prepared from the sol without PAA (Fig. 5a), whereas the films prepared with PAA have no cracks (Fig. 5b). SEM photographs of silica particles prepared with different amounts of PAA added are shown in Fig. 6. Monodispersed spherical particles are prepared at all concentrations of PAA. The particles prepared with PAA are much smaller than those of the particles prepared without PAA. The addition of PAA is thus proved to decrease the particle size and also to be useful for the formation of thick films without cracks by electrophoretic deposition of finer particles in the sols. The films consist of agglomerates of monodispersed silica particles with PAA. The deposition weight is considerably larger for the films with PAA than the films without PAA.

The generation of microcracks in the electrophoretically deposited silica films during the drying process is attributed to the shrinkage of the particles as well as the capillary force. It is thus important to control the surface activity and density of the silica particles to prepare thick films with no cracks. Heat treatment of the particles before electrophoretic deposition is expected to prevent cracking (Nishimori 1996b). The sols for electrophoresis were prepared by the redispersion of silica particles which were separated from the original sol obtained from a silicon alkoxide. The silica particles were heat-treated at various temperatures in air. The heat treatment of the particles at 600 °C prevented the generation of microcracks on the surface of the resultant films during the drying process. This is because rigid Si–O–Si networks in the particles were developed by the heat treatment at high temperatures and reduced the shrinkage of the deposited particles.

Since the isostatic point of silica is about pH 2–3 in water, the silica particles in sols have large negative charge at neutral and basic conditions. As a result, silica particles are usually deposited on an anode by applying DC voltage. However, anodic deposition has been pointed out to have disadvantages: elution of metal ions of the anode material into coating sols and incorporation of the eluted ions into films obtained. Such a contamination in the coating films sometimes causes the lowering of electric insulation and the coloration of the films. In contrast, cathodic deposition has been widely accepted in industry because these disadvantages can be avoided. A cationic polymer surfactant poly(ethylenimine) (PEI) is useful to control the surface charge of silica particles (Hasegawa et al. 1997). The surface charge of the silica particles can be reversed from negative to positive by adding a suitable amount of PEI at an appropriate value of pH. Thick films have been successfully prepared on the cathode by the electrophoretic deposition using PEI. The weight of the silica particles deposited on the cathode is maximized when the content of PEI added is 0.01 mass% and pH of the coating sols was 5. The decrease in the weight of the silica particles deposited at higher PEI contents than 0.01 mass% is caused by the H_2 generation at the cathode and the precipitation of silica particles in the sols.

The films prepared by the electrophoretic sol-gel deposition are basically composed of monodispersed spherical particles and have a lot of open spaces among these particles. If the open spaces are filled with some organic polymers, new type of inorganic–organic composite films with unique characteristics is expected to be obtained (Hasegawa et al. 1999). Silica particles are modified with 3-aminopropyltriethoxysilane (APS) and vinyltriethoxysilane (VTES). Smooth and crack-free films *ca.* 15 μm thick are obtainable when ASP-modified silica particles are used for cathodic deposition with addition of PEI. Thick films with reduced open spaces are obtained when VTES modified silica particles are co-deposited with polyethylene maleate.

Castro et al. have reported a new procedure for obtaining crack-free, protective, and glass-like coatings on metals, sintered at around 500 °C through electrophoretic deposition from particulate sol-gel suspensions (Castro et al. 2002). In this procedure, a particulate silica sol has been prepared under basic conditions by adding NaOH, where TEOS and methyltriethoxysilane (MTES) are mixed with NaOH in molar ratios of 0.3:1.2:0.2 and with H_2O/(TEOS + MTES) ratio less than stoichiometric. The resulting sol has a final pH of 9–10 and is diluted with absolute EtOH. The size of the particles developed from the synthesis is considered to be much less than 100 nm. The amount of deposited mass obtained by electrophoretic deposition depends on the particle concentration of the sol. For a constant concentration, the thickness of the deposits increases with an increase in current density. With the concentrated starting sol, the deposits as thick as 40 μm are obtained at 2.2 mA/cm^2. After drying, the maximum crack-free thickness is higher than 20 μm. When sintering of the coating is performed in air at 500 °C for 30 min, homogeneous, crack-free, and glass-like coatings are obtained up to 12 μm. The deposition time in the process is 5 min. Such a fast electrophoretic deposition kinetics inhibits the

substrate corrosion for the applied current densities. Potentiodynamic tests confirm the dielectric nature of the coating and its suitability for protecting metals.

A perfect electrophoretic self-assembly (EPSA) behavior of sol-gel derived silica microspheres into the layered pattern with the face-centered cubic structure has been observed (Louh and Huang 2007). EPSA technique has been demonstrated as an effective route to make various templates, which are associated with 3-D structures of silica microspheres in asymmetric geometries, for design of, for example, photonic crystals.

Since hydrophilic inorganic–organic composite films can be obtained through electrophoretic deposition using water solvent, the preparation of hydrophilic anode composed of platinum-deposited carbon and sol-gel silica nanospheres for proton exchange membrane fuel cells has recently been reported (Lo 2015). The films are hydrophilic; thus, they possess self-humidifying ability, leading to low-humidity long-term stability.

Titania Thick Films

Titania has been widely used as photocatalysts mostly in the form of thin films. If titania thick films are prepared in a simple process, the application field is expected to expand. Electrophoretic sol-gel deposition method has been applied to preparation of titania thick films. In preparation of titania particles, the particles tend to aggregate in the heat treatment process and the re-dispersion of the particles is difficult. However, hydrothermal treatment has been found to prevent the titania particles from aggregating, and titania thick films can be prepared by the electrophoretic sol-gel deposition using these hydrothermally treated particles (Sakamoto et al. 1998).

Titania particles are prepared by hydrolysis of titanium tetrabutoxide (TBOT). TBOT, distilled water, EtOH, and hydroxypropylcellulose (HPC) are used as starting materials, the molar ratio of TBOT/H_2O/EtOH being 1/7.5/100. HPC is dissolved in a half amount of EtOH, and then TBOT is added to the solution. Water and the rest of EtOH are mixed, and then the two solutions are mixed and stirred at 25 °C for 17 h. The titania particles formed in the solution are centrifuged and washed with EtOH by repeating the procedure of dispersion and centrifugation three times and then washed with H_2O in the same way. The particles are redispersed in H_2O and hydrothermally treated at 250 °C under 5 MPa for 1 h in an autoclave. The hydrothermally treated particles are separated by centrifugation and vacuum-dried. The resultant particles are heat-treated in air at 600 °C for 17 h.

The sols for electrophoretic deposition are prepared in the following procedure. The heat-treated titania particles are redispersed in EtOH and then added to a 1 mass% ammonia water containing PAA (m.w. = 450,000). The concentrations of titania and PAA are 1 and 0.1 mass% in the whole sol, respectively. The molar ratio of EtOH/H_2O is 8/2. By applying DC voltage on the electrodes immersed in the sol, the particles are electrophoresed to the anode to form a film. The anode as a coating

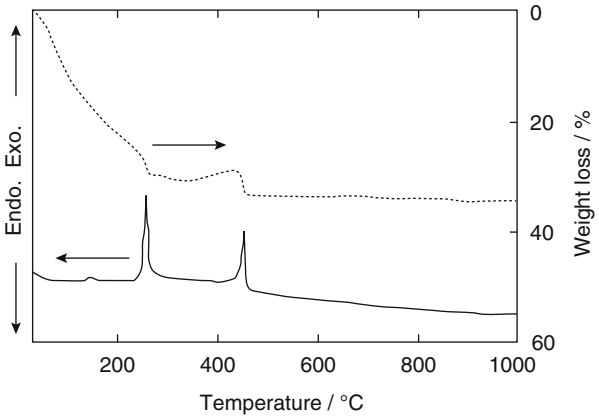

Fig. 7 DTA and TG curves of as-prepared titania particles before hydrothermal treatment (Sakamoto et al. 1998)

substrate is stainless steel sheet (SUS430, 40 × 25 × 1.0 mm^3), and the cathode as a counter electrode is spiral stainless steel wire (SUS304, 0.9 mm in diameter).

Differential thermal analysis (DTA) and thermogravimetry (TG) curves of as-prepared titania particles before being treated hydrothermally are shown in Fig. 7. The gradual weight loss is observed up to about 250 °C. This weight loss is due to evaporation of the solvent. Two exothermic peaks are observed at 250 °C and 450 °C in the DTA curve. The former peak is due to crystallization of titania. The latter, which is accompanied by slight weight loss in TG, is due to burning of residual organics.

XRD patterns of the particles before hydrothermal treatment for (a) as-prepared, (b) heat-treated at 350 °C, and (c) heat-treated at 600 °C are shown in Fig. 8. No diffraction peaks are observed in (a), whereas the pattern (b) shows diffraction peaks due to anatase. Therefore, the exothermic peak at 250 °C in DTA (Fig. 7) is due to crystallization of anatase. The XRD pattern of titania particles after the heat treatment at 600 °C shows that both anatase and rutile are present in the particles, indicating that the transformation from anatase to rutile occurs slowly. The activation energy for transformation from anatase to rutile is known to be rather high since breaking and reconstitution of Ti–O bonds are required. The transformation thus occurs at high temperatures, usually higher than 700 °C. In the present case, however, the chemical bond cleavage must occur by burning of residual organics, which produces a number of defects in the lattice. The presence of these defects probably makes it easier to reconstitute Ti–O bonds; the transformation from anatase to rutile thus occurs at such a low temperature.

XRD patterns of hydrothermally treated titania particles are shown in Fig. 9; (a) is for as-treated particles and (b) for the particles after heat-treated at 600 °C. By the hydrothermal treatment, the crystallization of amorphous titania particles occurs to form mainly anatase and a small amount of brookite as shown in (a); the transformation of these phases to rutile does not occur after the heat treatment at 600 °C for 17 h as shown in (b). DTA–TG curves of the hydrothermally treated titania particles

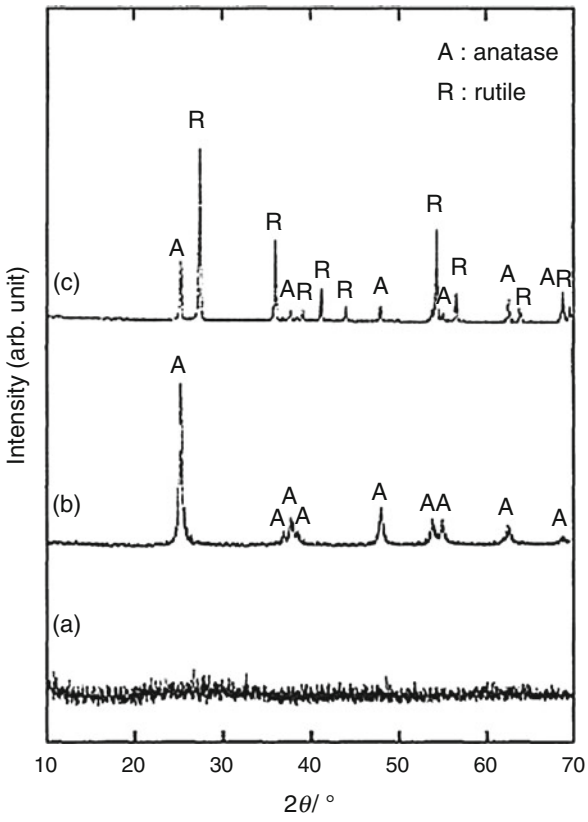

Fig. 8 XRD patterns of the particles before hydrothermal treatment for (**a**) as-prepared, (**b**) heat-treated at 350 °C, and (**c**) heat-treated at 600 °C (Sakamoto et al. 1998)

showed no exothermic peak or weight loss. Since the residual organics are probably eliminated during the hydrothermal treatment, the lowering of the transformation temperature does not occur.

SEM photographs of (a) as-prepared and (b) hydrothermally treated titania particles are shown in Fig. 10, both of which have been heat-treated at 600 °C for 17 h. The as-prepared particles aggregate in the heat treatment as shown in (a) and cannot be redispersed to prepare sols for the electrophoretic deposition. The aggregation is probably caused by the reconstitution of Ti–O bonds between the particles in the crystallization process. On the other hand, aggregation does not occur on the hydrothermally treated particles (b), indicating that the reconstitution of the bonds hardly occurs. The diameter of the particles is *ca.* 0.3 μm, which is almost the same as that of the as-prepared particles. The hydrothermally treated particles are easily redispersed in EtOH even after the heat treatment and homogeneous sols are obtained.

SEM photographs of the (a) surface and (b) cross section of a titania film deposited on a stainless steel sheet by electrophoresis are shown in Fig. 11. The applied voltage is 20 V and the deposition time is 30 min. The film consists of close-packed particles

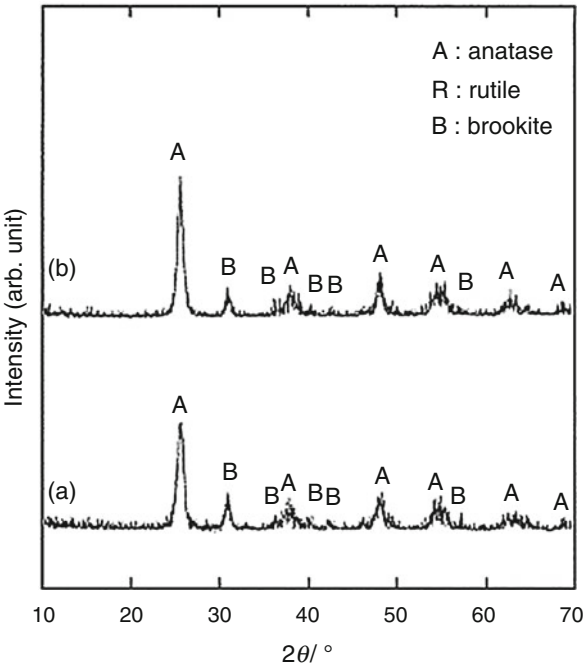

Fig. 9 XRD patterns of hydrothermally treated titania particles: (**a**) for as-treated particles and (**b**) for the particles after heat-treated at 600 °C (Sakamoto et al. 1998)

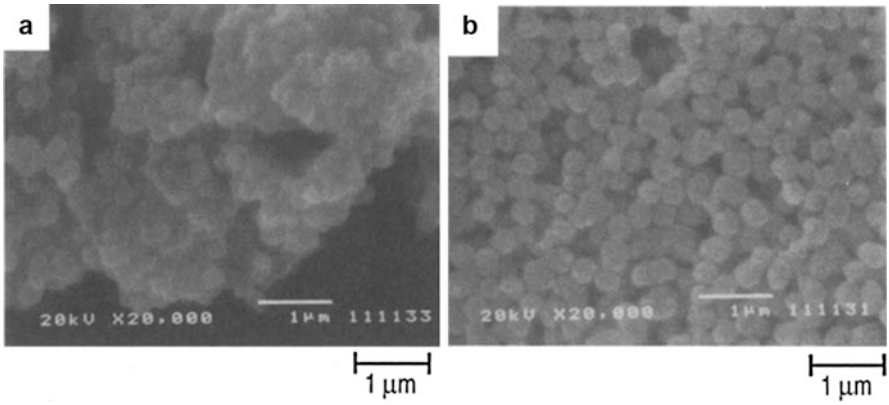

Fig. 10 SEM photographs of (**a**) as-prepared and (**b**) hydrothermally treated titania particles (Sakamoto et al. 1998)

and no cracks are observed. Crack-free films of *ca.* 20 μm in thickness are thus obtained.

Titania films have also been coated on glass foam substrates (Boccaccini et al. 2009). The used commercially available glass foams were lightweight, rigid insulating materials composed of closed cells with operating temperatures from −268 °C

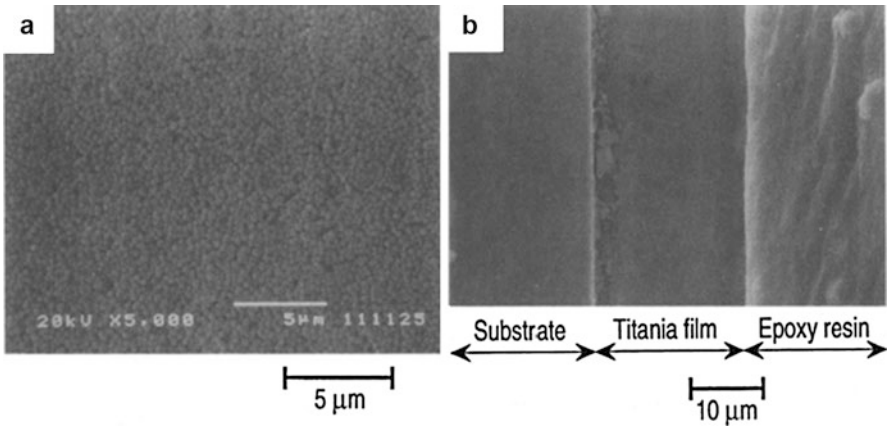

Fig. 11 SEM photographs of the (**a**) surface and (**b**) cross section of a titania film deposited on a stainless steel sheet by electrophoresis. The applied voltage was 20 V and the deposition time was 30 min (Sakamoto et al. 1998)

to 482 °C. Titania nanoparticles prepared by a sol-gel method were observed to migrate to the cathode encountering the glass foams in their trajectories and depositing on them. Titania-coated glass form would be of interest for some new lightweight products for photocatalytic and bio-related applications.

When titania particles are mixed with another material in solvent for electrophoretic deposition, titania composite thick films can be obtained. For instance, a thick film composed of titania nanoparticles and carbon nanotubes has been recently prepared through simultaneous electrophoretic deposition with an applied voltage of 80 V, followed by heating at 110 °C for 30 min (Bordbar et al. 2015).

Polysilsesquioxane Thick Films

The thick films prepared by the electrophoretic sol-gel deposition are composed of particles of submicrons in diameter, so that the films are usually opaque because of scattering of light at the interface between the particles and open spaces in the films. For example, in order to make such SiO_2 thick films transparent, the films should be sintered at temperatures higher than 1000 °C. This sintering temperature is, however, too high to apply the thick films obtained by the electrophoretic sol-gel deposition to optical devices because glass substrates could not withstand such a high temperature.

On the other hand, polysilsesquioxane ($RSiO_{3/2}$) derived from organoalkoxysilane, which has an organic group bonded to the silicon with a nonhydrolyzable covalent bond, has flexible structure since the amounts of bridging oxygens in $RSiO_{3/2}$ are smaller than those in SiO_2. Poly(phenylsilsesquioxane) ($PhSiO_{3/2}$) particles are morphologically changed from aggregates of the spherical particles to continuous layers with thermal sintering of the particles (Katagiri et al. 1998; Hasegawa et al. 2000). Accompanying the sintering, transparent thick films of a

few microns in thickness have been successfully prepared on the substrates by heating the electrophoretically deposited $PhSiO_{3/2}$ particles.

The hydrolysis and condensation of phenyltriethoxysilane (PhTES) are performed by the successive addition of HCl as an acid catalyst and NH_4OH as a base catalyst. In the first step, 0.01 mass% HCl is added to PhTES for hydrolysis and the mixture is stirred at 25 °C for 10 h until the mixture becomes homogeneous. In the second step, the resultant homogeneous solution is added to 4 mass% NH_4OH solution and stirred at 25 °C for additional 10 h for condensation of PhTES. The molar ratio of PhTES/H_2O (in HCl solution)/H_2O (in NH_4OH solution) is 1/20/180. The particles collected by centrifugation are washed by repeating redispersion in H_2O and centrifugation three times. The particles obtained are dried overnight at room temperature and then under vacuum at room temperature for 3 h.

Preparation procedure of sols for the electrophoretic is as follows. First, the particles are dispersed in 1 mass% NH_4OH solution with stirring. The solution is placed in an ultrasonic water bath to disperse the particles homogeneously. Second, after the particles are dispersed completely in NH_3 solution, EtOH is added to the solution. The molar ratio of H_2O (in NH_3 solution)/EtOH is 1/1. The amount of the particles added into the coating sols is 1 mass%.

Indium tin oxide(ITO)-coated glass is used as a substrate for coating to measure optical transmittance. Stainless steel spiral (SUS304BA) is used as a counter electrode. A constant DC voltage is applied between the two electrodes, i.e., the ITO-coated glass plate and the spiral, causing the electrophoresis of negatively charged $PhSiO_{3/2}$ particles toward the anode substrate (the ITO-coated glass plate).

Optical transmission spectra of ITO-coated glass substrates coated with $PhSiO_{3/2}$ thick films heat-treated at various temperatures are shown in Fig. 12. For comparison, the spectrum of an ITO-coated glass substrate without the film is also given (spectrum (f) in Fig. 12). Transmittance of the substrate with the $PhSiO_{3/2}$ thick film

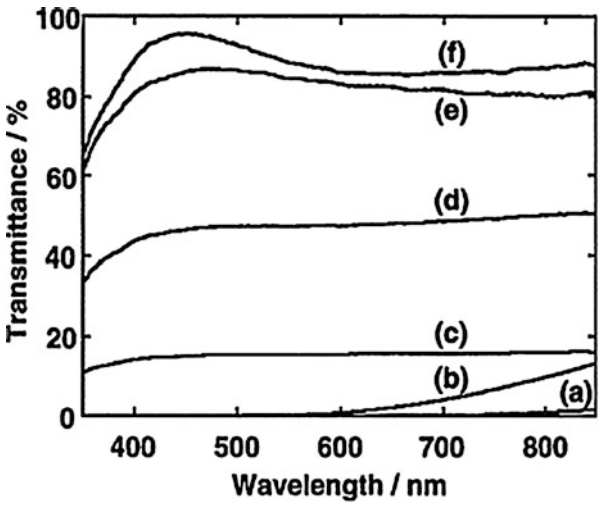

Fig. 12 Optical transmission spectra of ITO-coated glass substrates coated with $PhSiO_{3/2}$ thick films heat-treated at various temperatures: (**a**) for as-prepared film; (**b**–**e**) for the films heat-treated at 100 °C, 200 °C, 300 °C, and 400 °C, respectively; (**f**) for the ITO-coated glass substrate without the film (Hasegawa et al. 2000)

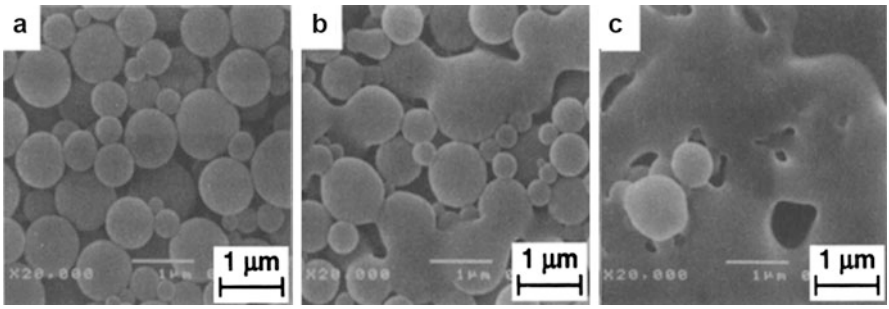

Fig. 13 SEM photographs of the $PhSiO_{3/2}$ particles heat-treated at various temperatures. (**a**–**c**) are for the particles heat-treated at 150 °C, 200 °C, and 250 °C, respectively. Heat-treatment time was fixed to be 30 min. The decrease of the interface is consistent with the result of the improvement of transparency, as shown in Fig. 12 (Hasegawa et al. 2000)

without heat treatment is <1% in the visible range (450–850 nm), as shown in spectrum (a). On the other hand, the transmittance of the substrate with the film increases as the heat-treatment temperature increases. After heat treatment at 400 °C for 2 h (spectrum (e)), transmittance of the coated substrate becomes as high as 85% in the visible range. Such a transparent thick film is promising for the application to optical devices.

SEM photographs of the $PhSiO_{3/2}$ particles heat-treated at various temperatures are shown in Fig. 13. Heat treatment of the $PhSiO_{3/2}$ particles is carried out by placing the particles into the electric furnace which is heated beforehand to each desired temperature. Heat-treatment time is 30 min at a given temperature. The shape of the spherical particles is still kept after a heat treatment at 150 °C (Fig. 13a). Morphological change is observed when the heat-treatment temperature reaches 200 °C (Fig. 13b). At this temperature, the neighboring particles begin to sinter each other to produce larger particles. The degree of the thermal sintering proceeds and much larger particles are produced at 250 °C (Fig. 13c). These photographs indicate that the higher the heat-treatment temperature, the easier the $PhSiO_{3/2}$ particles soften and change in morphology. As a result of the heat treatment and subsequent morphological change, the interface between the particles and open spaces among the particles decreases. The decrease of the interface is consistent with the result of the improvement of transparency, as shown in Fig. 12. From the thermal analysis, decomposition of the phenyl group in the $PhSiO_{3/2}$ particles is observed at temperatures near 500 °C. Consequently, the maximum heat treatment temperature is determined to be 400 °C.

Highly transparent films, as shown in the spectrum (e) in Fig. 12, are obtained only when heat treatment is carried out by placing thick films into the electric furnace which is heated beforehand to a temperature of 400 °C. In this heat treatment, it is important to heat the films to 400 °C in a very short time. On the other hand, only translucent or opaque films are obtained after the films are heated at a slow rate from room temperature to 400 °C, indicating that the heating rate is also another important factor to prepare transparent thick films.

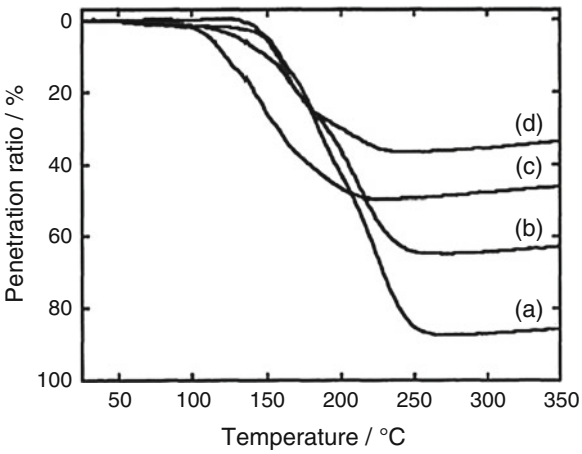

Fig. 14 Penetration ratio of the test probe at 0.5 g into the test samples against heat treatment temperature under various heating rates. Heating rates are (**a**) 20 °C/min, (**b**) 10 °C/min, (**c**) 1 °C/min, and (**d**) 1 °C/min with pre-heat treatment (Hasegawa et al. 2000)

The penetration ratio of the probe at 0.5 g into the test samples against temperature under various heating rates are shown in Fig. 14. Heating rates are (a) 20 °C/min, (b) 10 °C/min, (c) 1 °C/min, and (d) 1 °C/min; the test sample (d) is heat-treated at 100 °C for 2 h before the penetration test. Penetration ratio is defined as the percentage of penetration depth to thickness of the test sample. Regardless of the heating rate, penetration begins in the range of 100–150 °C and finishes at 200–250 °C. However, the final penetration ratio is different according to the heating rate; the higher the heating rate is, the larger the final penetration ratio becomes. From the penetration ratio measurement, the test sample becomes softest when the heating rate is highest, 20 °C/min, as shown in the curve (a) in Fig. 14. The reason for the decrease in the final penetration ratio with a decrease in the heating rate is that the test sample becomes rigid due to dehydration condensation during the longer heating. For the same reason, the pre-heat-treated test sample (curve (d) in Fig. 14) also has a low penetration depth because the sample possesses the rigid structure.

^{29}Si-CPMAS-NMR spectra of the $PhSiO_{3/2}$ particles (a) before and (b) after heat treatment at 400 °C for 2 h are shown in Fig. 15. Two peaks are observed at 69 and 78 ppm in the spectrum (a). The intensities of these two peaks are almost the same each other. These two peaks observed at 69 and 78 ppm are assigned to the T_2 and the T_3 units, respectively. Before heat treatment, the amount of T_2 unit, which behaves as a flexible unit, is almost the same as that of T_3 unit, which behaves as a rigid unit. However, after the heat treatment at 400 °C for 2 h, the T_2 unit disappears and only the T_3 unit is observed. This result supports the occurrence of the dehydration condensation during heat treatment, as described above. From such facts, the flexible T_2 unit which is present in the $PhSiO_{3/2}$ particles before heat treatment changes to the rigid T_3 unit during the heat treatment. Once the $PhSiO_{3/2}$ particles composed of only T_3 units are generated, these particles cannot be expected to soften or change in morphology by further heat treatment. Consequently, softening and morphological change of $PhSiO_{3/2}$ particles in thick films has to be achieved before the flexible T_2 units change completely to the rigid T_3 units.

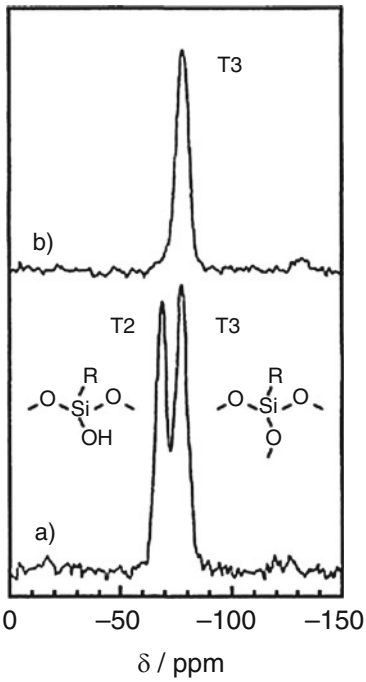

Fig. 15 ^{29}Si-CPMAS-NMR spectra of the $PhSiO_{3/2}$ particles (**a**) before and (**b**) after heat treatment at 400 °C for 2 h (Hasegawa et al. 2000)

SEM photographs of the surface of the $PhSiO_{3/2}$ thick films are shown in Fig. 16. The film without heat treatment is composed of aggregated spherical particles, and many open spaces among the particles and cracks are observed in Fig. 16a. In contrast, the shapes of the particles shown in Fig. 16b are indiscernible, but large dimples still remain in the film heat-treated at 200 °C for 2 h. This implies that the softening of the $PhSiO_{3/2}$ particles at 200 °C is not enough to achieve morphological change completely. The film heat-treated at 400 °C for 2 h becomes a monolith with neither open spaces nor dimples, as shown in Fig. 16c. These SEM photographs indicate that the increase in optical transmittance shown in Fig. 12 is due to the decrease in open spaces and cracks that cause light scattering. SEM photographs of the cross section of the $PhSiO_{3/2}$ thick films on ITO-coated glass substrates before and after heat treatment are shown in Fig. 17. The film is fixed with the epoxy resin for SEM observation of the film (Fig. 17a) before heat treatment because the films are very fragile. On the heat treatment at 400 °C (Fig. 17b), the films are adhered so strongly to the substrate. The thickness of the films decreases, from *ca.* 8 μm in Fig. 17a to *ca.* 3 μm in Fig. 17b, accompanied by the heat treatment at 400 °C for 2 h. This change of thickness is ascribed to the loss of open spaces among the particles by softening and viscous flow of the particles. Figure 17b shows that the film is homogenous in the direction of depth.

Several kinds of polysilsesquioxane particles have been prepared from organotriethoxysilanes and employed in the electrophoretic sol-gel deposition for the preparation of the transparent, thick films. Among the polysilsesquioxane

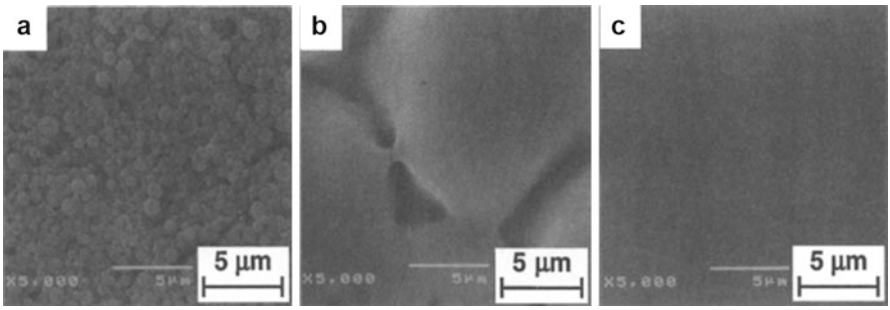

Fig. 16 SEM micrographs of the surface of the $PhSiO_{3/2}$ thick films (**a**) without heat treatment, (**b**) heat-treated at 200 °C and (**c**) 400 °C for 2 h (Hasegawa et al. 2000)

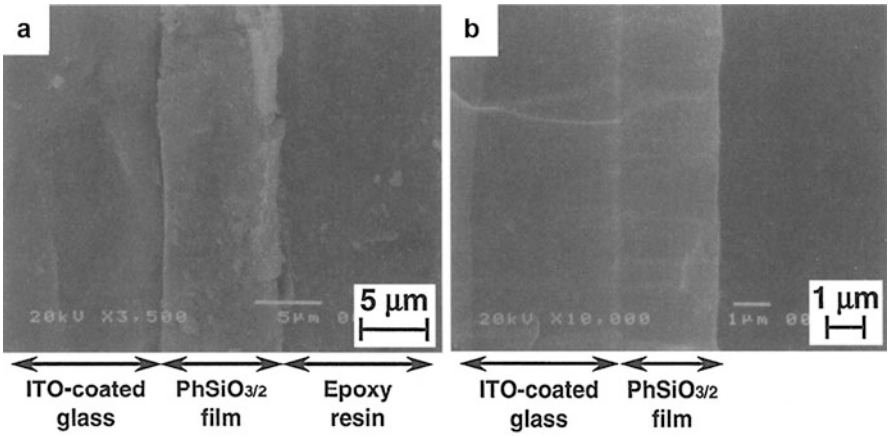

Fig. 17 SEM micrographs of the cross section of the $PhSiO_{3/2}$ thick films on ITO-coated glass substrates (**a**) before and (**b**) after heat treatment at 400 °C (Hasegawa et al. 2000)

particles prepared, poly(benzylsilsesquioxane) ($BnSiO_{3/2}$) particles derived from benzyltriethoxysilane (BnTES) are also found to sinter at lower temperatures than $PhSiO_{3/2}$ particles to form transparent thick films (Matsuda et al. 2000, 2001). The thermal sintering of the particles is a unique phenomenon for $PhSiO_{3/2}$ and $BnSiO_{3/2}$. Thus, the comparison of the thermal softening behavior for $PhSiO_{3/2}$ and $BnSiO_{3/2}$ particles affords useful information to control the sintering of organosilsesquioxanes for the fabrication of highly transparent, thick films in this process.

Gel permeation chromatography (GPC) elution curves of (a) $PhSiO_{3/2}$ and (b) $BnSiO_{3/2}$ particles are shown in Fig. 18. It can be seen that the GPC curve of $PhSiO_{3/2}$ (a) shows a broader band at shorter retain time than that of $BnSiO_{3/2}$ (b), indicating that $PhSiO_{3/2}$ consists of polymerized species with lager molecular weights than those in $BnSiO_{3/2}$ particles. The weight average molecular weight of the particles is evaluated to be 5.0×10^3 for $PhSiO_{3/2}$ and 2.2×10^3 for $BnSiO_{3/2}$ according to the polystyrene standard.

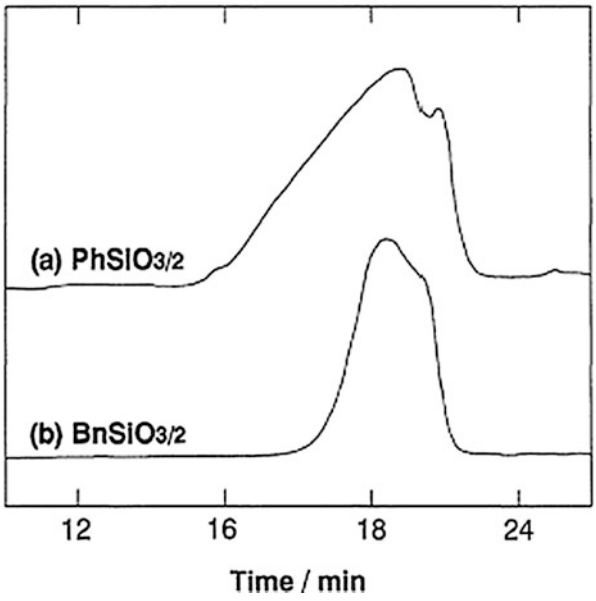

Fig. 18 GPC elution curves of (**a**) $PhSiO_{3/2}$ and (**b**) $BnSiO_{3/2}$ particles (Matsuda et al. 2000)

Morphological changes of $PhSiO_{3/2}$ and $BnSiO_{3/2}$ particles with heat treatment are shown in Fig. 19a–f. Figure 19a–c is SEM photographs for the $PhSiO_{3/2}$ particles before heat treatment, after heat treatment at 100 °C for 30 min, and at 140 °C for 30 min, respectively; Fig. 19d–f is for the $BnSiO_{3/2}$ particles before heat treatment, after heat treatment at 40 °C for 30 min, and at 50 °C for 30 min, respectively. The aggregates of spherical $PhSiO_{3/2}$ and $BnSiO_{3/2}$ particles of 0.2–1 μm in diameter are seen before heat treatment in Fig. 19a, d. Although the spherical shapes of the particles are kept after a heat treatment at 100 °C for $PhSiO_{3/2}$ (Fig. 19b) and at 40 °C for $BnSiO_{3/2}$ (Fig. 19e), necking among the particles is seen after a heat treatment at 140 °C for $PhSiO_{3/2}$ (Fig. 19c) and at 50 °C for $BnSiO_{3/2}$ (Fig. 19f). These results typically indicate that both of $PhSiO_{3/2}$ and $BnSiO_{3/2}$ particles are thermally softened and the on-set temperatures of the thermal sintering for $PhSiO_{3/2}$ and $BnSiO_{3/2}$ particles are about 140 °C and 50 °C, respectively.

The penetration ratios of $PhSiO_{3/2}$ and $BnSiO_{3/2}$ monoliths under a probe load of 0.5 g and a heating rate of 10 °C/min are shown in Fig. 20a, b, respectively. While the penetration ratio of $PhSiO_{3/2}$ increases to be about 60% at temperatures from 140 °C to 240 °C, the ratio slightly decreases from 240 °C to 400 °C. The increase in the penetration ratio reflects the softening and decrease in viscosity of $PhSiO_{3/2}$. The slight decrease from 240 °C to 400 °C can be ascribed to thermal expansion of hardened $PhSiO_{3/2}$ monolith on the glass substrate. The penetration begins at about 140 °C for $PhSiO_{3/2}$ regardless of the heating rate, whereas the ratio increases with an increase in the heating rate. On the other hand, the ratio of $BnSiO_{3/2}$ drastically increases at 47 °C to become about 90% at 100 °C and monotonically increases from 100 °C to 160 °C. These results of the penetration ratio measurements agree with the

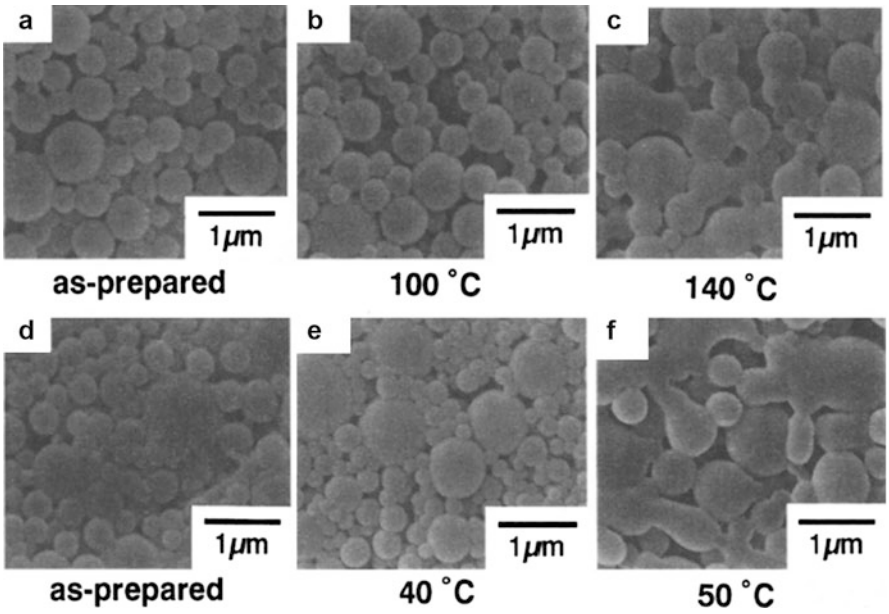

Fig. 19 (**a**–**c**) are SEM photographs for the $PhSiO_{3/2}$ particles before heat treatment, after heat treatment at 100 °C for 30 min, and at 140 °C for 30 min, respectively. (**d**–**f**) for the $BnSiO_{3/2}$ particles before heat treatment, after heat treatment at 40 °C for 30 min, and at 50 °C for 30 min, respectively (Matsuda et al. 2000)

morphological changes of the particles due to the fusion during the heat treatment and also suggest that the viscosity of the particles significantly decreases at these temperatures. The penetration ratio of $BnSiO_{3/2}$ is larger than that of the $PhSiO_{3/2}$, indicating that $PhSiO_{3/2}$ hardens during the heating. From the comparison of the penetration curves, the increase in the penetration ratio of $BnSiO_{3/2}$ during heating is more drastic than that of $PhSiO_{3/2}$, suggesting that the viscosity of $BnSiO_{3/2}$ is considerably lower than that of $PhSiO_{3/2}$ at temperatures around their on-set temperatures of the thermal sintering.

DSC heating curves of $PhSiO_{3/2}$ particles from 30 °C to 120 °C and $BnSiO_{3/2}$ particles from 30 °C to 70 °C on repeated runs are, respectively, shown in Fig. 21a, b. The thermal sintering between the particles is observed for both $PhSiO_{3/2}$ and $BnSiO_{3/2}$ particles after the repeated heating and cooling runs in the above temperature ranges, as expected from Fig. 20. Although an endothermic peak due to glass transition is clearly observed at around 100 °C in the first heating of $PhSiO_{3/2}$ particles, such a peak is not appreciable in the second and third runs. In contrast, an endothermic peak due to glass transition is observable at around 40 °C in ail the DSC curves of the repeated heating runs for the $BnSiO_{3/2}$ particles. These results indicate that the viscosity of the $PhSiO_{3/2}$ particles first decreases due to the thermal softening of the particles on heating at temperatures higher than the glass transition temperature and then the polymerization degree and distribution of the molecular

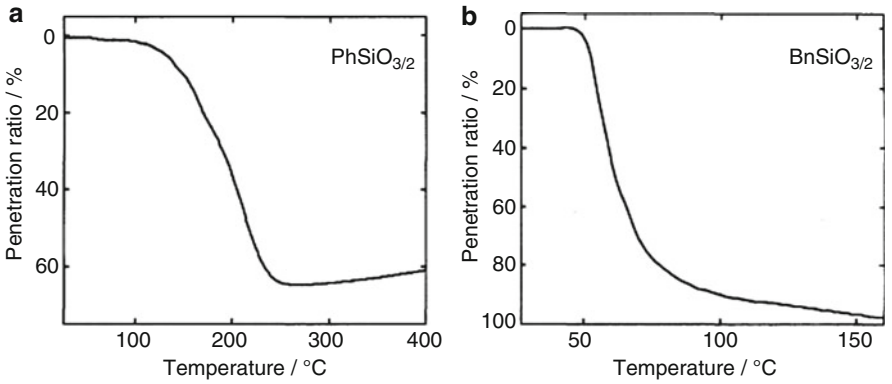

Fig. 20 Penetration ratios of (**a**) $PhSiO_{3/2}$ and (**b**) $BnSiO_{3/2}$ monoliths under a probe load of 0.5 g and a heating rate of 10 °C/min (Matsuda et al. 2000)

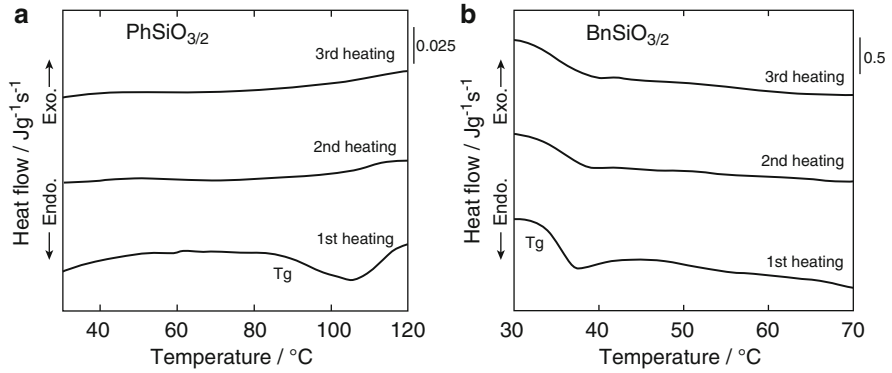

Fig. 21 DSC heating curves of (**a**) $PhSiO_{3/2}$ particles from 30 °C to 120 °C and (**b**) $BnSiO_{3/2}$ particles from 30 °C to 70 °C on repeated runs (Matsuda et al. 2000)

weight of the $PhSiO_{3/2}$ increases. These phenomena probably make the glass transition of $PhSiO_{3/2}$ particles unappreciable on the repeated heating and cooling runs. Glass transition is reversible for the $BnSiO_{3/2}$ particles, so that the polymerization degree and distribution of the molecular weight of the thermally sintered $BnSiO_{3/2}$ tend to remain constant at around on-set temperature for thermal sintering. The difference of changes in polymerization degree and distribution of the molecular weight at around the thermal sintering on-set temperature should provide the $PhSiO_{3/2}$ and $BnSiO_{3/2}$ particles with thermosetting and thermoplastic properties, respectively.

By taking the advantages of the physical properties of $BnSiO_{3/2}$, micropatterning of convex-shaped $BnSiO_{3/2}$ thick films has been prepared (Takahashi et al. 2006, 2007). $BnSiO_{3/2}$ particles were first electrophoretically deposited on ITO-coated substrates with a hydrophobic-hydrophilic micropatterned surface. Afterwards,

$BnSiO_{3/2}$ molten liquid on the hydrophobic areas migrated toward the hydrophilic areas by heating at the temperature above Tg of $BnSiO_{3/2}$, due to the difference in wettability on the substrates. Convex-shaped $BnSiO_{3/2}$ micropatterns with high transparency were formed on the hydrophilic areas.

Copolymerized $PhSiO_{3/2}$ and $BnSiO_{3/2}$ particles have been successfully prepared from their corresponding organotriethoxysilanes by the sol-gel method (Matsuda et al. 2002). Transparent thick films of a few microns in thickness are prepared on glass substrates with ITO-coatings by heat-treating the copolymerized particles which are electrophoretically deposited on the substrates. The on-set temperature for thermal sintering of the copolymerized particles monotonically decreases from 150 °C to 50 °C with increasing the $BnSiO_{3/2}$ content.

Template-Based Oxide Nanorods

The ability to form oxide nanorods is of great interest in a number of research areas. A unique method for using sol-gel electrophoresis in the formation of oxide nanorods has been demonstrated by Limmer et al. (2001, 2002). In the process, the template-based growth of nanorods of several oxides ceramics is formed by means of the sol-gel electrophoresis. Both single metal oxide (TiO_2, SiO_2) and complex oxides ($BaTiO_3$, $Sr_2Nb_2O_7$ and $Pb(Zr_{0.52}Ti_{0.48})O_3$) have been grown by this method. Uniformly sized nanorods of about 125–200 nm in diameter and 10 μm in length are grown over large area with unidirectional alignment. Oxide nanorods of desired stoichiometric chemical composition and crystal structure are readily achieved by an appropriate procedure of sol preparation, with a heat treatment for crystallization and densification.

In the formation of lead zirconate titanate (PZT) nanorods, lead acetate, titanium isopropoxide, zirconium *n*-propoxide, glacial acetic acid, lactic acid, ethylene glycol, and glycerol were used for the PZT sols. The template membranes used for the growth of nanorods were track-etched hydrophilic polycarbonate (PC) with pore diameters of 100 and 200 nm and a thickness of 10 μm. The PC membrane attached to Al cathode is placed in contact with the sol, and a potential of 5 V is applied between the cathode and the Pt anode. Samples thus obtained are dried at about 100 °C and heated to between 700 °C and 800 °C to both density and crystallize the PZT nanorods, as well as to burn off the PC membranes.

Polycrystalline $BaTiO_3$ nanorods have been synthesized with sol-gel electrophoretic deposition (EPD) into anodic aluminum oxide (AAO) templates (Žagar et al. 2011). A $BaTiO_3$ sol was prepared by dissolving barium acetate in glacial acetic acid, followed by an addition of titanium isopropoxide. Ethylene glycol was finally added to the solution in order to adjust the viscosity and to stabilize the sol. The AAO templates with pore diameters of approximately 200 nm and with a thickness of up to 60 mm were attached to an aluminum working electrode, and a Pt mesh electrode was used as the counter electrode. A potential of 30 V was applied and maintained for 30 min to ensure complete filling of the AAO template. After the EPD, the samples were annealed, then the AAO was removed by NaOH treatment.

Summary

The principle and the research progress in the electrophoretic sol-gel deposition technique, which is combined sol-gel method for particle preparation and electrophoretic deposition of the sol-gel derived particles, have been described. In the principal, (1) preparation of particles by the sol-gel method, (2) deposition of particles by electrophoresis, (3) constant-voltage and constant-current deposition, and (4) solvent and electrification are introduced. In the practical application, (1) silica thick films, (2) titania thick films, (3) polysilsesquioxane thick films, and (4) template-based oxide nanorods are illustrated. The electrophoretic sol-gel deposition technique offers the advantages of functional coatings in various research fields such as chemically and mechanically protective, electrically conductive, photocatalytic, and bioactive materials, and it expands the possibility of fabricating optical components and aligned micro- and nanostructures.

References

Boccaccini AR, Rossetti M, Roether JA, Zein SHS, Ferraris M. Development of titania coatings on glass foams. Construct Build Mater. 2009;23:2554–8.

Bordbar M, Alimohammadi T, Khoshnevisan B, Khodadadi B, Yeganeh-Faal A. Preparation of MWCNT/TiO_2-Co nanocomposite electrode by electrophoretic deposition and electrochemical study of hydrogen storage. Int J Hydrog Energy. 2015;40:9613–20.

Castro Y, Durán A, Moreno R, Ferrari B. Thick sol–gel coatings produced by electrophoretic deposition. Adv Mater. 2002;14:505–7.

Hamaker HC, Verwey EJ. The role of forces between the particles in electrophoretic deposition and other phenomena. Trans Faraday Soc. 1940;36:180–5.

Hasegawa K, Tatsumisago M, Minami T. Preparation of thick silica films by the electrophoretic sol–gel deposition using a cationic polymer surfactant. J Ceram Soc Jpn. 1997;105:569–72.

Hasegawa K, Kunugi S, Tatsumisago M, Minami T. Preparation of thick films by electrophoretic deposition using surface modified silica particles derived from sol–gel method. J Sol-Gel Sci Technol. 1999;15:243–9.

Hasegawa K, Katagiri K, Matsuda A, Tatsumisago M, Minami T. Effect of heat treatment on morphology and transparency of thick inorganic–organic hybrid films prepared by the electrophoretic sol–gel deposition of polyphenylsilsesquioxane particles. J Korean Ceram Soc. 2000;6:15–20.

Iler RK. The chemistry of silica. New York: Wiley; 1979.

Ishihara T, Sato K, Takita Y. Electrophoretic deposition of Y_2O_3-stabilized ZrO_2 electrolyte films in solid oxide fuel cells. J Am Ceram Soc. 1996;79:913–9.

Katagiri K, Hasegawa K, Matsuda A, Tatsumisago M, Minami T. Preparation of transparent thick films by electrophoretic sol–gel deposition using phenyltriethoxysilane-derived particles. J Am Ceram Soc. 1998;81:2501–3.

Kishida K, Tatsumisago M, Minami T. Preparation of thick silica films by combined sol–gel and electrophoretic deposition methods. J Ceram Soc Jpn. 1994;102:336–40.

Koura N, Tsukamoto T, Shoji H, Hotta T. Preparation of various oxide films by an electrophoretic deposition method: a study of the mechanism I. J Appl Phys. 1995;34:1643–7.

Kuwabara K, Sugiyama K, Ohno M. All-solid-state electrochromic device: 1. Electrophoretic deposition film of proton conductive solid electrolyte. Solid State Ion. 1991;44:313–8.

Limmer SJ, Seraji S, Forbess MJ, Wu Y, Chou TP, Nguyen C, Cao G. Electrophoretic growth of lead zirconate titanate nanorods. Adv Mater. 2001;13:1269–72.

Limmer SJ, Seraji S, Wu Y, Chou TP, Nguyen C, Cao G. Temperature-based growth of various oxide nanorods by electrophoresis. Adv Funct Mater. 2002;12:59–64.

Lo A-Y, Huang C-Y, Sung L-Y, Louh R-F. Electrophoretic deposited Pt/C/SiO_2 anode for self-humidifying and improved catalytic activity in PEMFC. Electrochim Acta. 2015;180:610–5.

Louh R-F, Huang E. Electrophoretic self-assembly of sol–gel derived silica microspheres. Solid State Phenom. 2007;124–126:599–602.

Matsuda A, Sasaki T, Hasegawa K, Tatsumisago M, Minami T. Thermal softening behavior of poly (phenylsilsesquioxane) and poly(benzylsilsesquioxane) particles. J Ceram Soc Jpn. 2000;108:830–5.

Matsuda A, Sasaki T, Hasegawa K, Tatsumisago M, Minami T. Thermal softening behavior and application to transparent thick films of poly(benzylsilsesquioxane) particles prepared by the sol–gel process. J Am Ceram Soc. 2001;84:775–80.

Matsuda A, Sasaki T, Tanaka T, Tatsumisago M, Minami T. Preparation of copolymerized phenylsilsesquioxane-benzylsilsesquioxane particles. J Sol-Gel Sci Technol. 2002;23:247–52.

Mizuguchi J, Sumi K, Muchi T. A highly stable nonaqueous suspension for electrophoretic deposition of powdered substances. J Electrochem Soc. 1983;130:1819–25.

Nagai M, Yamashita K, Umegaki T, Takuma Y. Electrophoretic deposition of ferroelectric barium-titanate thick-films and their dielectric-properties. J Am Ceram Soc. 1993;76:253–5.

Nishimori H, Tatsumisago M, Minami T. Preparation of thick silica films by the electrophoretic sol–gel deposition on a stainless steel sheet. J Ceram Soc Jpn. 1995;103:78–80.

Nishimori H, Hasegawa K, Tatsumisago M, Minami T. Preparation of thick films in the presence of poly(acrylic acid) by using electrophoretic sol–gel deposition. J Sol-Gel Sci Technol. 1996a;7:211–6.

Nishimori H, Tatsumisago M, Minami T. Heat-treatment effect of dispersed particles on the preparation of thick silica films by using electrophoretic sol–gel deposition. J Mater Sci. 1996b;31:6529–33.

Nishimori H, Tatsumisago M, Minami T. Growth mechanism of large monodispersed silica particles prepared from tetraethoxysilane in the presence of sodium dodecyl sulfate. J Sol-Gel Sci Technol. 1997;9:25–31.

Nojima H, Shintaku H, Nagata M, Koba M. Fabrication of Ag-doped $YBa_2Cu_3O_{7-x}$ superconducting films on Cu substrates by electrophoretic deposition. J Appl Phys. 1991;30: L1166–8.

O'Brien RW, White LR. Electrophoretic mobility of spherical colloidal particle. J Chem Soc, Faraday Trans 2. 1978;74:1607–14.

Pierre AC. Introduction to sol–gel processing. Boston: Kluwer; 1998.

Ryan W, Massoud E. Electrophoretic deposition could speed up ceramic casting. Interceramics. 1979;2:117–9.

Sakamoto R, Nishimori H, Tatsumisago M, Minami T. Preparation of titania thick films by electrophoretic sol–gel deposition using hydrothermally treated particles. J Ceram Soc Jpn. 1998;106:1034–6.

Sarker P, Nicholson PS. Electrophoretic deposition (EPD): mechanisms, kinetics, and application to ceramics. J Am Ceram Soc. 1996;79:1987–2002.

Stern O. Zur Theore der elektrischen doppelschicht. Z Elektrochem. 1924;30:508.

Stöber W, Fink A, Bohn E. Controlled growth of monodisperse silica spheres in the micron size range. J Colloid Interface Sci. 1968;26:62–9.

Takahashi K, Tadanaga K, Hayashi A, Tatsumisago M. Micropatterning of transparent poly (benzylsilsesquioxane) thick films prepared by the electrophoretic sol–gel deposition precess using a hydrophobic-hydrophilic-paterned surface. J Am Ceram Soc. 2006;89:3832–5.

Takahashi K, Tadanaga K, Matsuda A, Hayashi A, Tatsumisago M. Fabrication of convex-shaped polybenzylsilsesqujioxane micropatterns by the electrophoretic sol–gel deposition process using

indium tin oxide substrates with a hydrophobic-hydrophilic-patterned surface. J Sol-Gel Sci Technol. 2007;43:85–91.

Yamashita K, Nagai M, Umegaki T. Fabrication of green films of single- and multi-component composites by electrophoretic deposition technique. J Mater Sci. 1997;31:6661–4.

Yamashita K, Yonehara E, Ding XF, Hamagami J, Umegaki T. Electrophoretic coating of multi-layered apatite on alumina ceramics. J Biomed Mater Res. 1998;43:46–53.

Žagar K, Rečnik A, Šturm S, Gajović A, Čeh M. Structural and chemical characterization of $BaTiO_3$ nanorods. Mater Res Bull. 2011;46:366–71.

Zhang Y, Brinker CJ, Crooks RM. Electrophoretic deposition of sol–gel-derived ceramic coatings. In: Hampden-Smith MJ, Brinker CJ, Klemperer WG, editors. Proceedings of Materials Research Society Symposium, 1992 Apr 27–May 1; San Francisco; 1992. Better ceramics through chemistry V, vol. 271. p. 465–70.